This is a post-peer-review, pre-copyedit version of an article published in *Journal of Flow Chemistry*.
The final authenticated version is available online at: http://doi.org/10.1007/s41981-021-00204-y

Graphical abstract

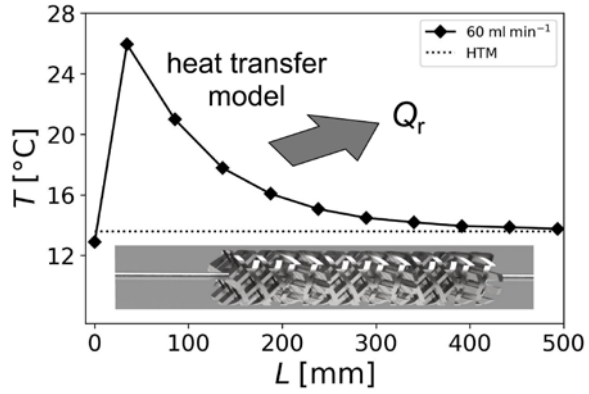

Type of article

Full paper

Title

Continuous milli-scale reaction calorimeter for direct scale-up of flow chemistry

Author information

M.Sc. ETH Marlies Moser (corresponding author)

Fluitec mixing + reaction solutions AG

Seuzachstrasse 40

8413 Neftenbach, Switzerland

mm@fluitec.ch

ORCID: 0000-0003-0386-9492

Dipl.-Ing. HTL Alain G. Georg

Fluitec mixing + reaction solutions AG

Seuzachstrasse 40

8413 Neftenbach, Switzerland

B.Sc. Finn L. Steinemann

ZHAW Zurich University of Applied Sciences

School of Engineering

Institute of Materials and Process Engineering, Technikumstrasse 9

8401 Winterthur, Switzerland

ORCID: 0000-0003-1918-7920

Dr. David P. Rütti

ZHAW Zurich University of Applied Sciences

School of Engineering

Institute of Materials and Process Engineering, Technikumstrasse 9

8401 Winterthur, Switzerland

ORCID: 0000-0002-1789-4085

Dr. Daniel M. Meier

ZHAW Zurich University of Applied Sciences

School of Engineering

Institute of Materials and Process Engineering, Technikumstrasse 9

8401 Winterthur, Switzerland

ORCID: 0000-0001-5806-2130

Abstract

Reaction calorimetry of flow processes is important for scale-up and safety in flow chemistry. Due to the increasing number of flow processes, corresponding flow calorimeters are required as an alternative or addition to high-precision batch calorimeters. In this work, a milli-scale isoperibol continuous flow calorimeter was used to measure the heat of reaction based on an elaborated heat transfer model. This allows for reaction calorimetry without calibration. The model was tested with a selective, fast and exothermic neutralization reaction of acetic acid and sodium hydroxide at different flow rates, concentrations and viscosities. Deviations of the mean heats of reaction from the literature values were only about 2 %. The calorimetric data can further be used for direct scale-up with tube bundle mixer heat exchangers having similar heat transfer characteristics. In addition, a reaction screening at different flow rates allows to find the maximum temperature and maximum heat generation. This data is useful in safety analyses of continuous processes. For these reasons, continuous reaction calorimetry provides a practical scale-up tool for flow processes.

Keywords

Continuous flow reactor

Isoperibolic reaction calorimetry

Heat of reaction

Safety

Process development

Scale-up

Declarations

Availability of data and material

At Fluitec for the next 10 years

Code availability

At Fluitec

Ethics approval

Not applicable

Consent to participate

Yes

Consent for publication

Yes

Article Highlights

- Flow calorimetry was achieved for a fast and selective reaction without the need for calibration
- The mean heat of reaction of the flow screening deviates only about 2 % from the literature value
- Low pressure drop in the milli-scale flow reactor allows the use of high viscous process fluids

1 Introduction

Reaction calorimetry is a key requirement for chemical process engineering and scale-up design. Traditionally, calorimetry has been conducted in well characterized batch calorimeters usually under isothermal conditions [1, 2]. While batch calorimeters are the choice for engineering and scale-up of chemical processes in stirred tank reactors, continuous flow calorimeters are required for scaling flow chemistry.

Until today, only a few flow calorimeters have been described in literature and even fewer are commercially available [3]. Most of them are microreactor-like and work under almost isothermal conditions [3–10]. While micro-calorimeters are suitable to mimic microreactors, they are limited in describing flow chemistry at larger scale. Unlike in the numbering-up approach, in the sizing-up approach of tubular reactors, non-isothermal behavior could be experienced [11]. For this application, Mortzfeld *et al.* have described for the first time flow reaction calorimetry in milli-reactors (V = 17 ml) [12]. With their method, they found only 4 % deviations of the determined heat of reaction compared to commercial batchwise calorimeter experiments by studying selective model reactions. However, for non-selective reactions, deviations from batch to continuous flow calorimeters were significantly higher. This finding strongly implies the need for investigating flow chemistry in accordingly designed flow calorimeters to be economical and safe in chemical production.

Mortzfeld *et al*. [12] applied a comprehensive calibration procedure to find the overall heat transfer coefficient k. In contrast, herein we present a novel approach without the need for calibration. It is based on calculations using the precise description of the heat transfer in the tubular reactor (V = 44.3 ml). This method enables an economic and fast reaction screening in flow reactors. In addition to the determined heat of reaction, the temperature profile can be elucidated and used for a further scale-up. The surface to volume ratio of the used plug flow reactor (PFR) is so as to be scaled-up by Fluitec tube bundle mixer heat exchangers by keeping the surface to volume ratio constant [13]. The aim of this kind of reaction calorimetry is mainly providing a reliable scale-up tool for flow processes and thus increase their safety at higher scales, which is still a current topic [14].

In this work, a selective and fast neutralization reaction was examined aiming to verify the heat transfer model described by Georg *et al*. [15]. The neutralization reaction of acetic acid (AcOH) with sodium hydroxide (NaOH) – a common model reaction in flow calorimetry [4, 7] – was used to determine the heat of reaction at different flow rates, concentrations and viscosities.

2 Material and methods

2.1 Experimental setup

The experimental setup used is schematically shown in Fig. 1. The heart of the continuous reaction calorimeter consists of a jacketed tubular reactor (L = 500 mm, D_i = 12.3 mm, V_{void} = 44.3 ml, Contiplant PFR-50-SS, Fluitec mixing + reaction solutions AG, Switzerland) [13, 15], which is equipped with static mixers and an axial temperature sensor (D = 1.6 mm) with 10 thermocouples (Class 1, Type K) (Fig. 2). The reaction chamber contains a premixer section (CSE-X, D_i = 4.7 mm) followed by a residence time section (CSE-X, D_i = 12.3 mm). Two flow-controlled dosing systems (DZRP-200, 63639, Fluitec), containing gear pumps and Coriolis mass flow meters, were connected to the entry of the PFR. For measuring the initial fluid temperatures, a temperature sensor (Class A, Pt-100, 53286, Fluitec) was positioned in the fluid storage tank. A back pressure valve (Contiplant valve, 64144, Fluitec) was placed at the reactor outlet, ensuring a constant back pressure.

As heat transfer medium (HTM) water was recirculated through the outer shell of the reactor driven by a heating-cooling thermostat (Ministat, Peter Huber Kältemaschinenbau AG, Germany). A Coriolis mass flow meter (Promass 80F15, Endress+Hauser (Schweiz) AG, Switzerland) was used to measure its flow rate. Two temperature sensors (Class A, Pt-100, 53286, Fluitec) were placed on the heat transfer medium side to measure the inlet and outlet temperatures. A picture of the reaction calorimeter set-up can be found in the Supplementary Information.

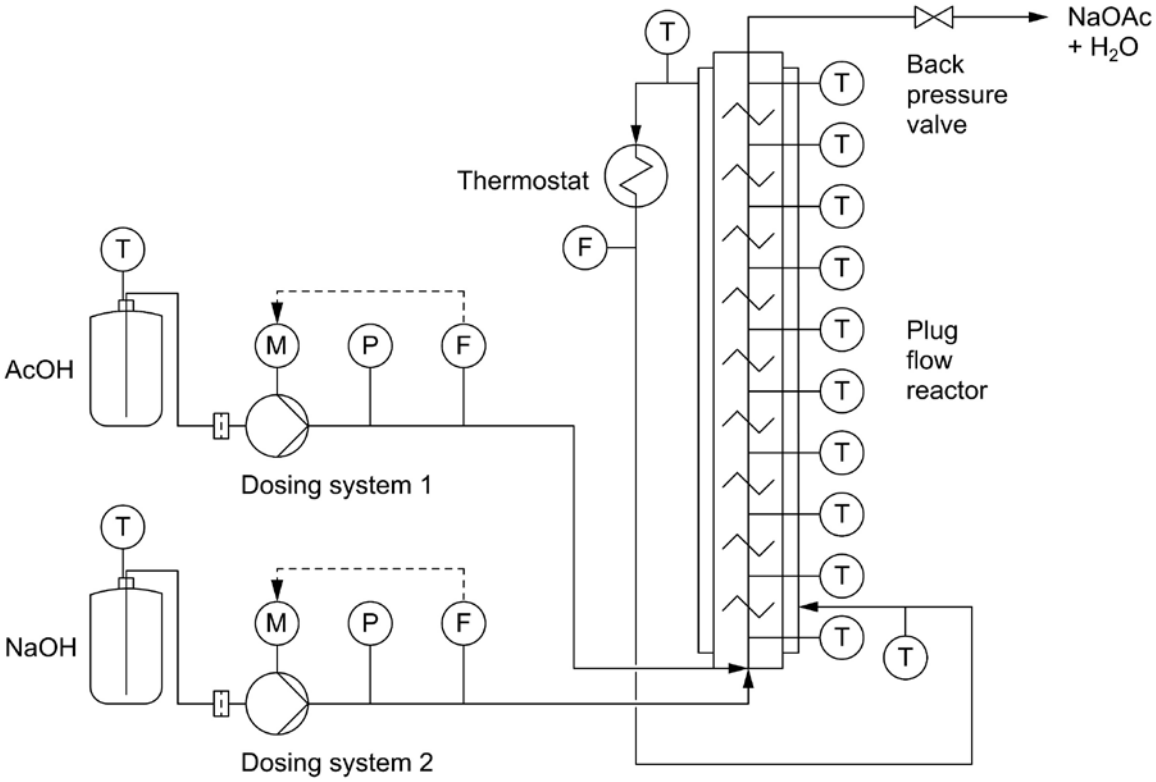

Fig. 1 Scheme of the continuous reaction calorimeter set-up

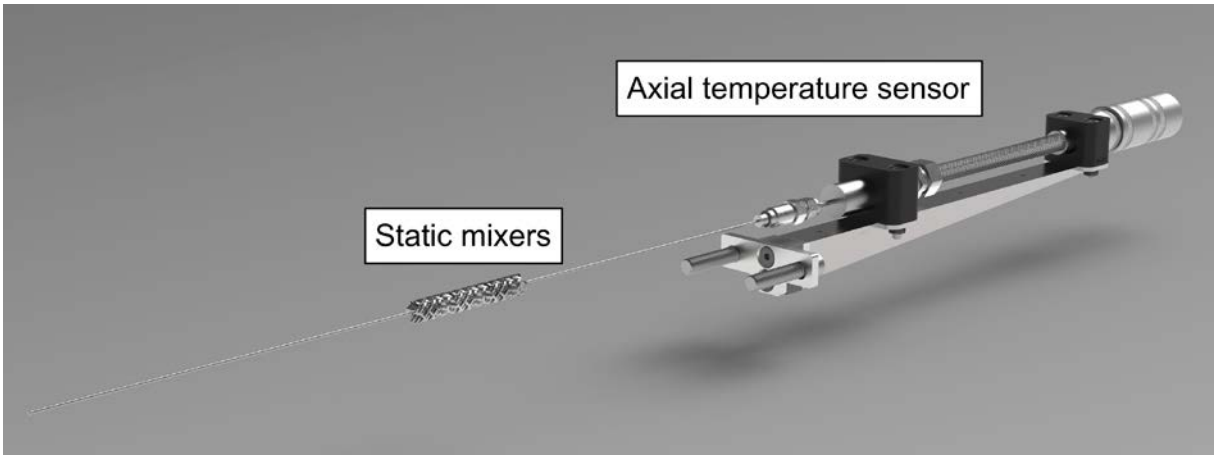

Fig. 2 Illustration of the temperature sensor (10 measuring points) placed at the center of the static mixers inside the PFR

Data were recorded continuously at 1 s time intervals by means of an inhouse designed Siemens S7 control system. Prior to experiments, each thermocouple of the axial temperature sensor was temperature adjusted. Therefore, the water-filled reactor was heated to 10, 20, 30, 40, 50, 60, 70 and 80 °C.

2.2 Neutralization reaction

The neutralization of acetic acid with sodium hydroxide has been chosen as a model reaction because it is selective, very fast, highly exothermic and has already been investigated with continuous flow calorimeters [4, 7] (Eq. 1).

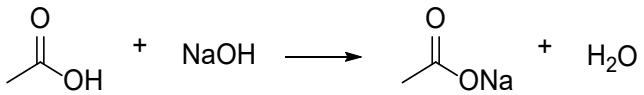

(1)

In order to determine the total heat of reaction, the residence time τ has to be longer than the reaction time. Since a neutralization reaction in water is almost instantaneous, its reaction time is very small [16]. This model reaction

could therefore be classified as type A reaction according to Roberge *et al*. [17], with a reaction half-life $t_{1/2}$ << 1 s. Thus, the reaction time is only limited by the mixing time. The relations of the time constants are given in Eq. 2.

$$t_{1/2} << t_{mix} < \tau \quad (2)$$

Solutions of 2 and 4 molar (M) acetic acid (100 %, Carl Roth AG, Switzerland) and sodium hydroxide (> 99 %, Carl Roth AG, Switzerland) were prepared with distilled water (0.4 mS m^{-1} conductivity at 25 °C, Förch AG, Switzerland). Both solutions, acid and base, were equimolarly fed in the PFR with flow rates of 10, 20, 30, 40 and 50 ml min^{-1} each. Temperatures were recorded after an equilibration phase of at least three residence times and 20 measuring points were averaged. The measurements have been reproduced using fresh reactant solutions.

For the experiments at higher viscosity (140 mPas), 70 vol% glucose syrup (HAGLUC.806.C800, Hostettler-Spezialzucker AG, Switzerland) was added to the acetic acid solution. Experiments with 2 molar solutions of acetic acid and sodium hydroxide were carried out at 10, 20, 25, 30 and 40 ml min^{-1} each.

2.3 Experimental procedure

Prior to the continuous reaction calorimeter experiment, a batch experiment was performed and the temperature increase monitored. For this reason, a 100 ml glass bottle filled with 50 ml NaOH solution was stirred with a magnetic stirrer at 400 rpm and 50 ml AcOH solution was added and the temperature increase was measured using a Pt-100 temperature sensor. Adiabatic conditions were assumed, whereas the heat absorption of the glass was considered.

Subsequently, the flow experiments were conducted. The HTM temperature was set to the actual room temperature and the mass flow rate to approximately 500 kg h^{-1}. After tempering for 30 min the first data point was acquired. The inner tube was flushed with water and reactants at a high flow rate (100 ml min^{-1}) to remove possible air inclusions. While the system was running, the back pressure was set to 1 bar. The dosing flow rates were then set to the target values and kept constant for at least three residence times before recording the data. At steady state, the pH value was measured at the outlet of the reactor to ensure the completion of the neutralization reaction. After the measurement, the entire system was flushed with water at a high flow rate.

The fully converted reaction mixtures were analyzed for their density, viscosity, thermal conductivity and specific heat capacity. Density measurements were conducted in a 100 ml volumetric flask with an analytical balance (WBA-620, Witeg Labortechnik GmbH, Germany). Viscosity was determined by means of a viscosimeter (Viscolite 700, Hydramotion Ltd, England). Thermal conductivity and specific heat capacity were measured using a corresponding measurement system (Lamda, Flucon fluid control GmbH, Germany).

2.4 Determination of the heat of reaction

Determination of the heat of reaction is based on the theory of a co-current heat exchanger and isoperibolic heat flow calorimetry. The overall heat balance is described in Eq. 3. At steady state, the time-dependent change of heat will be zero. Assuming the heat of neutralization as the only source of heat, the heat flow of the reaction $\dot{Q}_r$ is the sum of the heat flow exchanged $\dot{Q}_{ex}$ and the heat flow not exchanged $\dot{Q}_{nex}$.

$$0 = \frac{dQ}{dt} = \dot{Q}_r - \dot{Q}_{ex} - \dot{Q}_{nex};\ \dot{Q}_r = \dot{Q}_{ex} + \dot{Q}_{nex} \quad (3)$$

The exchanged heat flow $\dot{Q}_{ex}$ is calculated segment-wise according to the general heat exchanger formula (Eq. 4).

$$\dot{Q}_{ex} = \sum_{j=1}^{n} k_j \cdot A_{a,j} \cdot \Delta T_j \quad (4)$$

Where k_j is the local overall heat transfer coefficient (calculated using Eq. 7 - 11), $A_{a,j}$ the heat exchanger surface at the outside of the tube and ΔT_j the difference of the local temperature to the temperature of the heat transfer medium.

Not exchanged heat flow $\dot{Q}_{nex}$, resulting in the local temperature rise, is also summed-up segment-wise according to Eq. 5.

$$\dot{Q}_{nex} = \sum_{j=1}^{n} \dot{m} \cdot c_p \cdot \Delta T_j \quad (5)$$

Where $\dot{m}$ represents the total mass flow rate of the reaction mixture, c_p the specific heat capacity and ΔT_j the temperature difference within one segment.

Finally, the specific heat of reaction Q_r is obtained by dividing the total heat flow of the reaction by the total mass flow rate, as shown in formula Eq. 6.

$$Q_r = \frac{\dot{Q}_r}{\dot{m}} \quad (6)$$

Due to the well-insulated PFR and working at room temperature, heat exchange with the environment was neglected. The absorption of the heat by static mixers and tubes was taken into account by determining the *Nu*-*Pe* correlation (Eq. 9) with the same equipment as the determination of the heat of reaction.

The heat transfer coefficient *k* is obtained by heat transfer models as schematically shown in Fig. 3.

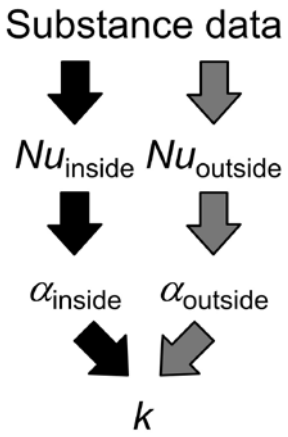

Fig. 3 Scheme of the determination of the overall heat transfer coefficient *k*

Accurate substance and process data, as the velocity *w*, inner diameter of the tube D_i, specific heat capacity c_p, density ρ, viscosity η and thermal conductivity λ of the reaction mixture, are required to calculate the Péclet number *Pe* and Prandtl number *Pr* in the inside of the tube as described in Eq. 7 and Eq. 8.

$$Pe = \frac{w \cdot D_i \cdot c_p \cdot \rho}{\lambda} \quad (7)$$

$$Pr = \frac{c_p \cdot \eta}{\lambda} \quad (8)$$

Applying the *Nu*-*Pe* correlation (Eq. 9) [15] leads to corresponding Nusselt numbers *Nu*. Viscosity differences of the core and wall are considered by the quotient of the *Pr* and Pr_W numbers.

$$Nu = 3.89 \cdot Pe^{0.32} \cdot \left(\frac{Pr}{Pr_W}\right)^{0.14} \quad (9)$$

The *Nu* number is transformed to the heat transfer coefficient α according to Eq. 10.

$$\alpha_i = Nu \cdot \frac{\lambda_i}{D_i} \quad (10)$$

The corresponding outer heat transfer coefficient α_a is calculated according to the ring-slit-correlations of VDI Wärmeatlas [18]. Together with the wall thickness *s*, the thermal conductivity of the wall λ_W and the outer A_a, inner A_i heat transfer surface and averaged to A_m, the corresponding overall heat transfer coefficient is obtained as described in Eq. 11.

$$k = \frac{1}{\frac{1}{\alpha_a} + \frac{s \cdot A_a}{\lambda_W \cdot A_m} + \frac{A_a}{\alpha_i \cdot A_i}} \quad (11)$$

The heat of reaction out of the reaction enthalpy ΔH_r and the concentration $c_{A,0}$ is calculated according to Eq. 12.

$$Q_r = \frac{-\Delta H_r \cdot c_{A,0}}{\rho} \quad (12)$$

The heat of reaction out of the adiabatic temperature rise ΔT_{ad} is calculated as described in Eq. 13.

$$Q_\mathrm{r} = \Delta T_\mathrm{ad} \cdot c_\mathrm{p} \qquad (13)$$

3 Results and discussion

The results of continuous reaction calorimetry at milli-scale based on the work of [12] and extended to an efficient, time-saving, non-calibrated approach is shown in this section. The prerequisite for calorimetry without calibration is a heat exchanger characterized with appropriate models.

3.1 Temperature profile

Temperature profiles of the fast and exothermic neutralization reaction at 2 M reactant concentrations measured by applying flow rates from 20 to 100 ml min^{-1} are shown in Fig. 4. The pH-measurements at the tubular reactor outlet confirmed complete neutralization (pH = 7.5). Due to the premixer, the reaction immediately started at the beginning of the tubular reactor. This resulted in a temperature maximum at the first temperature measuring point for all flow rates.

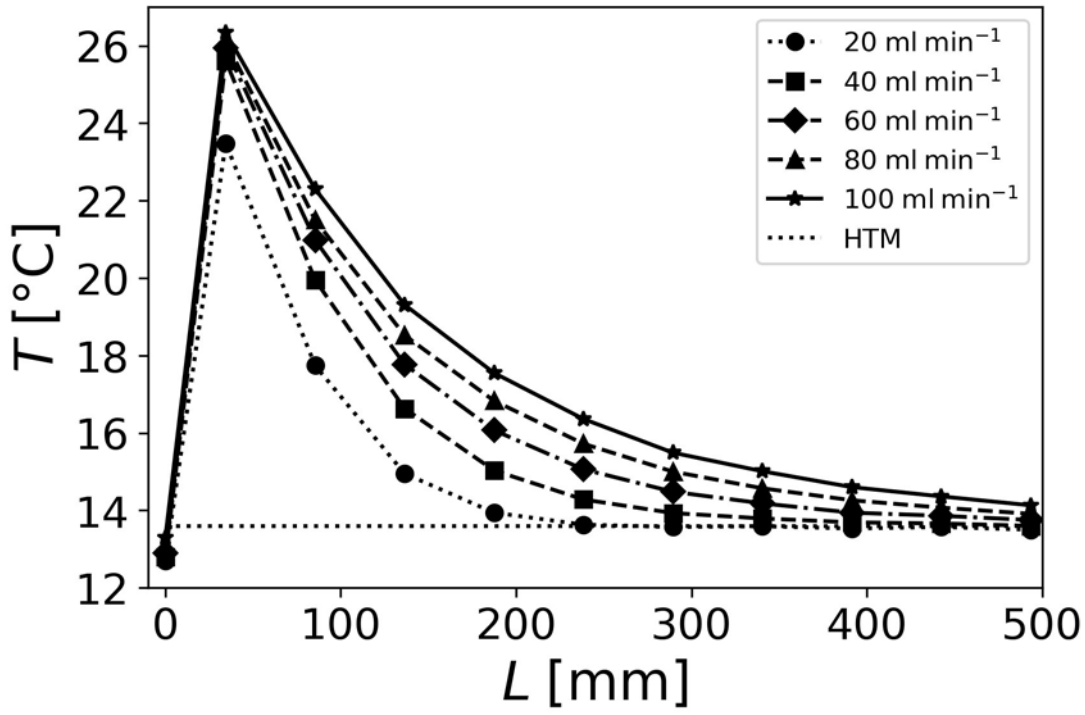

Fig. 4 Temperature profile of 2 M AcOH and 2 M NaOH at flow rates from 20 – 100 ml min^{-1}. T(HTM) = 13.6 °C

The maximum temperature at 20 ml min^{-1} was significantly lower than at higher flow rates, resulting from the lower local heat production. In general, for safety considerations, it is suggested to screen investigated reactions at different flow rates to identify the maximum temperature and maximum heat generation under flow conditions. The knowledge of the maximum temperature peak gives information about possible initiation of side reactions. Exothermic side reactions can be detected by an increased Q_r value, which is not the case for the selective neutralization reaction.

3.2 Determination of the heat of reaction

The heat of reaction was determined segment-wise by means of heat balances according to Eqns. 3 – 11. It could be assumed that the total heat determined originated from the neutralization reaction only. Thus, the heat of reaction Q_r would more precisely be named as the heat of neutralization. This corresponds to the enthalpy of formation of 1 mole of water and is defined as -57.4 kJ mol^{-1} [19]. Using formula Eq. 12, results in 55.3 kJ kg^{-1} and 106.6 kJ kg^{-1} for the 2 M and the 4 M solutions, respectively. The measured heats of reaction at different flow rates and concentrations along with the batch and literature values are given in Tab. 1. Batch experiments match within a maximum deviation of 2 %, implying the correct reactant solution concentrations. Regarding the flow measurements, the variation within a measurement series was calculated to ± 10 % and ± 12 % for the 2 M and 4 M experiments, respectively. Though the mean Q_r value was found to differ only 2 % and 0.2 % from their

corresponding literature values. The best accuracy was achieved with a total flow rate of 60 ml min^{-1}, where the percentage deviation from the literature value was 1 % for the 2 M experiments and 3 % for the 4 M experiments.

Tab. 1 Heat of reaction of the neutralization of AcOH with NaOH, 2 M and 4 M, at different flow rates compared to the batch and literature values [19]

Flow rate, $\dot{V}$ [ml min^{-1}]	Heat of reaction, Q_r, 2 M [kJ kg^{-1}]	Heat of reaction, Q_r, 4 M [kJ kg^{-1}]
20	65.0	125.5
40	59.3	113.0
60	56.0	103.0
80	52.5	97.4
100	50.1	93.3
Mean ± SD	56.6 ± 5.9	106.4 ± 13.0
Batch	55.7	104.0
Literature [19]	55.3	106.6

Hence, we conclude that the heat transfer model applied in this work (Eq. 9) well predicts the heat of reaction for the investigated neutralization reaction at the applied flow rate range. However, the heats of reaction were slightly overestimated at flow rates below 60 ml min^{-1} and underestimated at flow rates above 60 ml min^{-1}. The reason for these deviations lies mainly in the description of the heat transfer of the inner space. It was found that the heat transfer model is most robust for a range of *Pe* numbers from 700 - 800, which was calculated for the experiments at 60 ml min^{-1}. Moreover, the reason for the high accuracy at 60 ml min^{-1} was attributed to the rheological properties at this operating point. The flow velocity was calculated to be 8 mm s^{-1}, which is in the slowly laminar flow regime (Reynolds number Re = 72 and 49 for the 2 M and the 4 M solutions, respectively) and from experience highly suitable for tubular reactors with static mixers at milli-scale (CSE-X, D_i = 12.3 mm).

3.3 Evaluation for high viscous solutions

Due to its design, the milli-scale reaction calorimeter is suitable for higher viscous fluids, which is reflected in the low pressure drop. For example with the neutralization reaction mixture in 35 vol% glucose syrup (η = 7.3 mPas) at 80 ml min^{-1} the pressure drop was calculated to be only 17 mbar. At the beginning of the reaction section, 2 M AcOH in 70 vol% glucose syrup (η = 140 mPas) and 2 M NaOH in water (η = 1.7 mPas) were mixed. Therefore it is likely that stripes of high and low viscous liquids occur in the first section of the calorimeter which could affect the heat transfer. Such non-ideal behavior is addressed in the last term of Eq. 9 $(Pr/Pr_W)^{0.14}$ [20]. It describes viscosity differences at the wall and the inner space.

It was found that this factor needs to be considered for high viscous solutions because without considering the viscosity differences, i.e. η_W/η = 1, the mean Q_r value (60.9 kJ kg^{-1}) is 20 % higher than the literature value (49.8 kJ kg^{-1}). Since the average ratio η_W/η over the entire heat exchanger was not known, the heat of reaction could not be calculated straight forward. However, it was assumed that the neutralization reaction was complete (pH = 6, slightly acidic because of glucose) and selective. Therefore, a range of reasonable η_W/η was assumed and the heat of reaction was calculated and compared with the theoretical value (Fig. 5). A maximum ratio of wall viscosity to core viscosity averaged over the reactor of 140:7.3 was chosen, which corresponds to the ratio of the initial viscosity of the glucose solution and the viscosity of the final mixture. The mean Q_r value at the maximum viscosity ratio of η_W/η = 19 was calculated to be 44.5 kJ kg^{-1} which is 10 % below the literature value. The best agreement with the theoretical Q_r value was at η_W/η = 7 (49.7 kJ kg^{-1}). This finding highlights the relevance of the accurate substance data of the feed as well as of the product solutions for non-calibrated calorimetry.

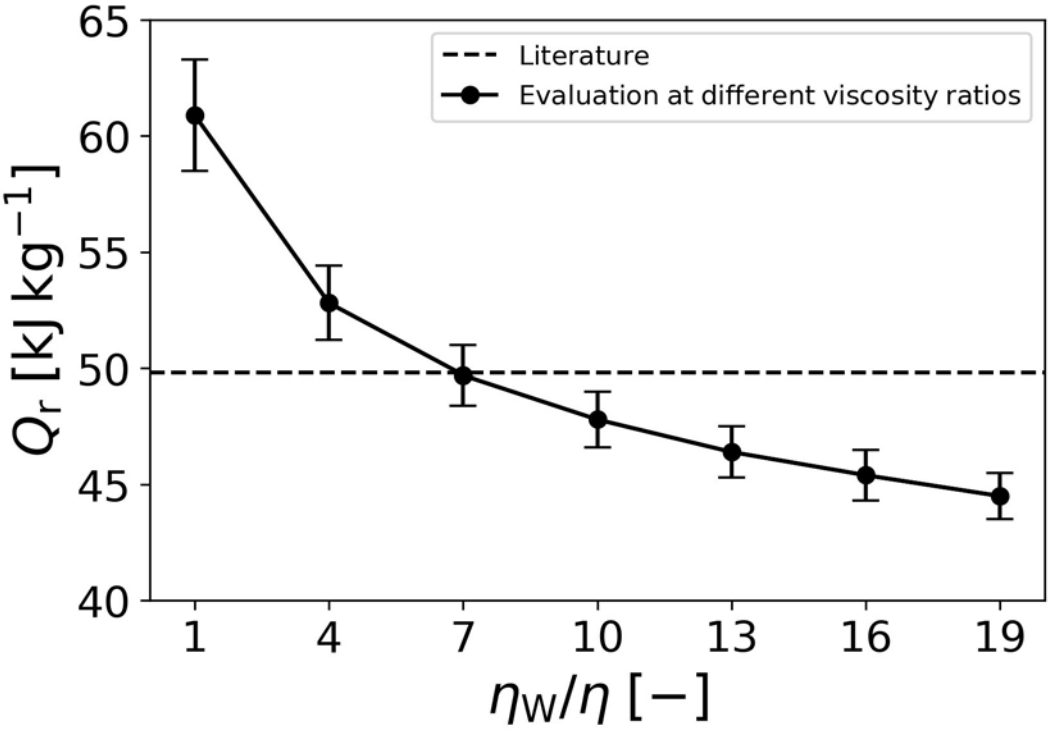

Fig. 5 Calculated heat of reaction of the neutralization in 35 vol% glucose with respect to viscosity differences of the wall and the inner space (η_W/η). Error bars refer to the standard deviation of experiments at different flow rates

3.4 Factors influencing accuracy

The main influencing factors of the heat-transfer-model-based isoperibolic flow reaction calorimetry are summarized in Fig. 6. It was found that deviations in temperatures have a great influence, while deviations in substance data have a minor influence on the calculated heat of reaction. However, the higher the heat of reaction, the lower the influence of temperature deviations.

In the case of higher viscous liquids or polymerization reactions, viscosity differences or fouling can occur and thus affect the heat transfer model or even reduce the reactor volume due to persistent deposits. Further influencing factors could be feed dosing inaccuracies and mixing limitations. The former was considered by flow-controlled dosing systems and the latter by a premixer (D_i = 4.7 mm) at the beginning of the reaction section.

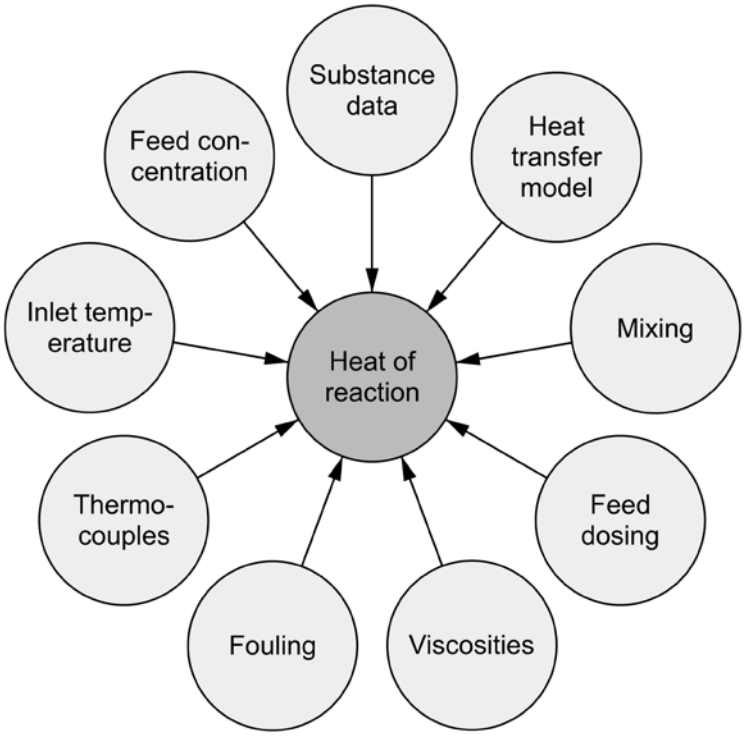

Fig. 6 Factors influencing the determination of the heat of reaction in continuous flow calorimetry

The heat transfer model was found to have a great influence on the calculated heat of reaction. Many similar heat transfer correlations have been applied [11, 21], but the correlation described in Eq. 9 provided the most robust solution for the flow rates, concentrations and viscosities used with the neutralization reaction. The perfect operating point with other fluids and reactions might be at other flow rate ranges. This is one reason why a screening of different flow rates is suggested. A further reason is the safety analysis, as a screening reveals the maximum temperature and the highest possible heat generation in case of a deviation in dosing of the feed solutions. It is particularly relevant for non-selective reactions.

3.5 Flow vs. batch calorimetry

The results of the neutralization reaction are compared with the similarly conducted flow calorimetry results described by Mortzfeld *et al.* [12] (Fig. 7). They carried out lithiation and Li-proton exchange reactions, whose batch references were conducted in a commercially established RC1 batch calorimeter [22]. Moreover, these results were obtained upon a calibration with inert fluids to find the k values. Whereas in this work the k values were calculated according to heat transfer models as described above.

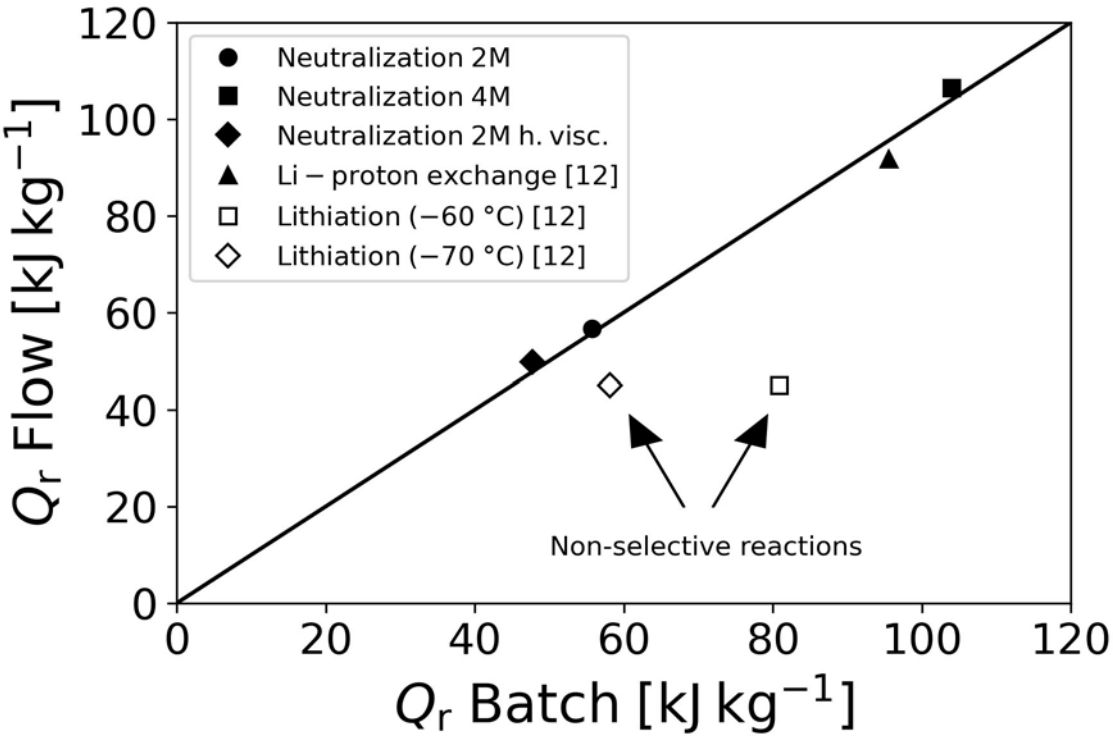

Fig. 7 Comparison of the heat of reaction determined in flow and batch operation for selective (diagonal) and non-selective reactions [12]. h.visc. = high viscous

Measuring points on the diagonal represent selective reactions whose Q_r values are not influenced by the reactor system or temperature. This applies for the neutralization reaction as well as for the Li-proton exchange. In contrast, the lithiation reaction was found to be non-selective when carried out in semi-batch mode. Due to the long residence time in the tank reactor, exothermic side reactions have been initiated which increased the measured heat of reaction. These side reactions could have been reduced at very low temperatures (- 70 °C) [12]. The fact that the heat of reaction is sensitive to the reactor system and temperature highlights again the importance of flow calorimetry in process development of flow processes.

In order to estimate the operating range of continuous flow calorimetry, a flow factor β is suggested (Eq. 14). Experience has shown that more accurate results are obtained at high heat generation and high flow rates than at low heat generation and low flow rates. The product of both parameters should therefore compensate for the inaccuracies at low flow rates and low heat of reaction. It was found that the β value should be at least 200 for accurate continuous flow calorimetry using the equipment presented herein.

$$\beta = \dot{V} \cdot \Delta T_{\mathrm{ad}} > 200 \qquad (14)$$

The flow rate in ml min^{-1} and the adiabatic temperature increase in °C are used. Considering the β flow factor enables calorimetry for processes with high adiabatic temperature rises at correspondingly low flow rates and vice versa. Further, it is suggested to apply flow conditions with *Re* numbers below 100, since the heat transfer model is best described in that range.

4 Conclusion and outlook

A continuous reaction calorimeter, similar to that described in [12], was used to determine the heat of reaction. Thereby, it was shown that the heat of reaction of the fast and exothermic neutralization reaction could be determined with the non-calibrated isoperibolic flow calorimeter with a deviation of the mean heat of reaction to literature values of maximum 2 %. Highest accuracies were achieved at 60 ml min^{-1} (w = 8 mm s^{-1}). The *Nu-Pe* function used to obtain k was successfully applied for the neutralization reaction at different concentrations and viscosities.

In the future, milli-scale flow calorimetry will be merged with the approach of continuous determination of reaction kinetics with the loop reactor as described in Rütti *et al.* [23]. This allows to determine reaction parameters for a

scale-up in a completely continuous way. Furthermore, the reaction calorimeter could be extended with suitable online analytics (e.g. IR or UV spectroscopy) at the outlet to determine the conversion of very slow reactions.

Application fields of this kind of continuous reaction calorimetry are in safety engineering as well as in process development for scale-up of flow chemistry. Regarding the safety analysis, always the worst case, meaning the experiment resulting in the highest temperature peak and greatest heat of reaction, should be considered. Therefore, a screening over a set of flow rates is recommended, which further allows to study the impact of possible dosing errors. The milli-scale flow calorimeter provides therefore a tool for direct scale-up of flow process with similar flow reactors regarding the heat-exchange properties, like the Fluitec tube bundle mixer heat exchanger [13]. This allows to keep the temperature profile constant during scale-up. Overall, the model-based isoperibolic continuous reaction calorimetry offers a fast way to obtain the heat of reaction of flow processes.

5 Acknowledgments

The authors thank the Swiss Government and Innosuisse for their funding and Berthold Schenkel, Francesco Venturoni, Bertrand Guélat, Jutta Polenk, Paolo Filipponi and Frederik Mortzfeld from Novartis Pharma AG for helpful discussions.

6 Funding

Co-funded by Innosuisse

7 Declarations

7.1 Conflicts of interest/Competing interests

The authors have no conflicts of interest to declare that are relevant to the content of this article.

7.2 Symbols

A_a, heat transfer surface at the outside of the tube [m^2]; A_i, heat transfer surface at the inside of the tube [m^2]; A_m, mean heat transfer surface [m^2]; $c_{A,0}$, initial concentration of the limiting reactant A [mol m^{-3}]; c_p, specific heat capacity [J kg^{-1} K^{-1}]; D, diameter [m]; D_i, inner diameter [m]; ΔH_r, reaction enthalpy [J mol^{-1}]; k, overall heat transfer coefficient [W m^{-2} K^{-1}]; L, length [m]; $\dot{m}$, mass flow rate [kg s^{-1}]; Q, heat [J]; $\dot{Q}_{ex}$, exchanged heat flow [W]; $\dot{Q}_{nex}$, not exchanged heat flow [W]; Q_r , specific heat of reaction [J kg^{-1}]; $\dot{Q}_r$, heat flow of reaction [W]; s, wall thickness [m]; t, time [s]; $t_{1/2}$, reaction half-life [s]; t_{mix}, mixing time [s]; T, temperature [K]; ΔT, temperature difference [K]; ΔT_{ad}, adiabatic temperature rise [K]; V, volume [m^3]; V_{void}, void volume [m^3]; $\dot{V}$, volume flow rate [m^3 s^{-1}]; w, flow velocity [m s^{-1}]

7.3 Dimensionless numbers

Nu, Nusselt number [-]; Nu_{inside}, Nusselt number in the tube [-]; $Nu_{outside}$, Nusselt number in the shell [-]; Pe, Péclet number [-]; Pr, Prandtl number [-]; Pr_W, Prandtl number at the wall [-]; Re, Reynolds number [-]

7.4 Greek symbols

α, heat transfer coefficient [W m^{-2} K^{-1}]; α_{inside}, α_i, heat transfer coefficient in the tube [W m^{-2} K^{-1}]; $\alpha_{outside}$, α_a, heat transfer coefficient in the shell [W m^{-2} K^{-1}]; β, flow factor [ml min^{-1} °C]; η, viscosity [Pa s]; η_W, viscosity at the wall [Pa s]; λ, thermal conductivity [W m^{-1} K^{-1}]; λ_W, thermal conductivity of the wall [W m^{-1} K^{-1}]; ρ, density [kg m^{-3}]; τ, residence time [s]

7.5 Abbreviations

AcOH, acetic acid; H_2O, water; h. visc., high viscous; HTM, heat transfer medium; M, molar; NaOAc, sodium acetate; NaOH, sodium hydroxide; PFR, plug flow reactor; SD, standard deviation; VDI, Verein Deutscher Ingenieure

8 References

1. Zogg A, Stoessel F, Fischer U, Hungerbühler K (2004) Isothermal reaction calorimetry as a tool for kinetic analysis. Thermochim Acta 419:1–17. https://doi.org/10.1016/j.tca.2004.01.015

2. Sarge SM, Höhne GWH, Hemminger W (2014) Calorimetry: fundamentals, instrumentation and applications. WILEY-VCH Verlag GmbH & Co. KGaA, Weinheim

3. Antes J, Gegenheimer M, Krause H, Löbbecke S, Wirker R, Knorr A (2008) Ortsaufgelöste Reaktionskalorimetrie in mikrostrukturierten Reaktoren. Chemie Ing Tech 80:1270–1270. https://doi.org/10.1002/cite.200750657

4. Reichmann F, Millhoff S, Jirmann Y, Kockmann N (2017) Reaction calorimetry for exothermic reactions in plate-type microreactors using seebeck elements. Chem Eng Technol 40:2144–2154. https://doi.org/10.1002/ceat.201700419

5. Frede TA, Dietz M, Kockmann N (2021) Software-guided microscale flow calorimeter for efficient acquisition of thermokinetic data. J Flow Chem. https://doi.org/10.1007/s41981-021-00145-6

6. Glotz G, Knoechel DJ, Podmore P, Gruber-Woelfler H, Kappe CO (2017) Reaction Calorimetry in Microreactor Environments - Measuring Heat of Reaction by Isothermal Heat Flux Calorimetry. Org Process Res Dev 21:763–770. https://doi.org/10.1021/acs.oprd.7b00092

7. Maier MC, Leitner M, Kappe CO, Gruber-Woelfler H (2020) A modular 3D printed isothermal heat flow calorimeter for reaction calorimetry in continuous flow. React Chem Eng 5:1410–1420. https://doi.org/10.1039/d0re00122h

8. Zhang C, Zhang J, Luo G (2020) Kinetics determination of fast exothermic reactions with infrared thermography in a microreactor. J Flow Chem 10:219–226. https://doi.org/10.1007/s41981-019-00071-8

9. Ładosz A, Kuhnle C, Jensen KF (2020) Characterization of reaction enthalpy and kinetics in a microscale flow platform. React Chem Eng 5:2115–2122. https://doi.org/10.1039/d0re00304b

10. Laudadio G, Gemoets HPL, Hessel V, Noël T (2017) Flow synthesis of diaryliodonium triflates. J Org Chem 82:11735–11741. https://doi.org/10.1021/acs.joc.7b01346

11. Dong Z, Wen Z, Zhao F, Kuhn S, Noël T (2021) Scale-up of micro- and milli-reactors: An overview of strategies, design principles and applications. Chem Eng Sci 10:100097. https://doi.org/10.1016/j.cesx.2021.100097

12. Mortzfeld F, Polenk J, Guélat B, Venturoni F, Schenkel B, Filipponi P (2020) Reaction calorimetry in continuous flow mode: A new approach for the thermal characterization of high energetic and fast reactions. Org Process Res Dev 24:2004–2016. https://doi.org/10.1021/acs.oprd.0c00117

13. Georg A, Däscher MB (2005) Chemische Reaktionen in Rohrreaktoren und statischen Mischern - Homogenität, Verweilzeitverhalten, Wärmeabfuhr, Auslegung, Anwendungsbeispiele. Chem Ing Tech 77:681–693. https://doi.org/10.1002/cite.200407095

14. Kockmann N, Thenée P, Fleischer-Trebes C, Laudadio G, Noël T (2017) Safety assessment in development and operation of modular continuous-flow processes. React Chem Eng 2:258–280. https://doi.org/10.1039/C7RE00021A

15. Georg A, Moser M, Merkel N, Rosasco E, Andreoli S, Hodler M (2020) Kontinuierliches Reaktionskalorimeter. EP20183838.0

16. Eigen M, De Maeyer L (1955) Untersuchungen über die Kinetik der Neutralisation. I. Zeitschrift für Elektrochemie 59:986–993. https://doi.org/10.1002/bbpc.19550591020

17. Roberge DM, Ducry L, Bieler N, Cretton P, Zimmermann B (2005) Microreactor technology: A revolution for the fine chemical and pharmaceutical industries? Chem Eng Technol 28:318–323. https://doi.org/10.1002/ceat.200407128

18. Verein Deutscher Ingenieure (2006) VDI-Wärmeatlas, 10th ed. Springer, Berlin, Heidelberg

19. Riedel E, Meyer H-J (2013) Allgemeine und Anorganische Chemie, 11th ed. De Gruyter, Berlin, Boston

20. Zlokarnik M (2002) Scale-up in chemical engineering. Wiley-VCH Verlag GmbH, Weinheim

21. Thakur RK, Vial C, Nigam KDP, Nauman EB, Djelveh G (2003) Static mixers in the process industries - a review. Chem Eng Res Des 81:787–826. https://doi.org/10.1205/026387603322302968

22. Toledo M (2021) Reaction Calorimeter RC1. https://www.mt.com/int/en/home/products/L1_AutochemProducts/Reaction-Calorimeters-RC1-

HFCal/RC1mx-Reaction-Calorimeter.html#overviewpm. Accessed 5 Jun 2021

23. Rütti DP, Moser M, Georg AG, Spier ES, Meier DM (2021) Kinetic data for continuous processes from liquid-liquid loop reactor experiments. Chem Ing Tech 93:1267–1272. https://doi.org/10.1002/cite.202100005